The effect of the band structure on the Voc value of ternary planar heterojunction organic solar cells based on pentacene, boron subphthalocyanine chloride and different electron acceptors

Z. El Jouad, E.M. El-Menyawy, G. Louarn, L. Arzel, M. Morsli, M. Addou, J.C. Bernède, L. Cattin

The effect of the band structure on the Voc value of ternary planar heterojunction organic solar cells based on pentacene, boron subphthalocyanine chloride and different electron acceptors.

Z. El Jouad,[1,5] E.M. El-Menyawy,[2,3] G. Louarn,[2] L. Arzel,[2] M. Morsli,[4] M. Addou,[5] J. C. Bernède[1*] and L. Cattin[2*]

[1]MOLTECH-Anjou, CNRS, UMR 6200, Université de Nantes, 2 rue de la Houssinière, BP 92208, Nantes, F-44000 France.
[2] Institut des Matériaux Jean Rouxel (IMN), CNRS, UMR 6502, Université de Nantes, 2 rue de la Houssinière, BP 32229, 44322 Nantes cedex 3, France.
[3] Solid State Electronics Laboratory, Solid State Physics Department, Physics Research Division, National Research Centre, 33 El-Bohouth St., Dokki, Giza 12622, Egypt.
[4] Université de Nantes, Faculté des Sciences et des Techniques, 2 rue de la Houssinière, BP 92208, Nantes, F-44000 France.
[5]Laboratoire Optoélectronique et Physico-chimie des Matériaux, Université Ibn Tofail, Faculté des Sciences BP 133 Kenitra 14000, Morocco.

Abstract

Using three organic materials in the cascade configuration of organic photovoltaic cells (OPVs) broadens the absorption range of visible light, resulting in an increase in the short circuit current density (Jsc). Herein, we report for the first time the use of three organic molecules, pentacene, boron subphthalocyanine chloride (SubPc) and fullerene (C_{60}). Upon comparison with the binary pentacene/C_{60} and SubPc/C_{60}structures, the high Jsc value obtained for the ternary structure induces an increase in the OPV efficiency. This improvement is limited by the small open circuit voltage (Voc) value due to the low absolute value of the highest occupied molecular orbital of pentacene. Our experimental study confirmed that the Voc is ultimately limited by the energy levels of the outer layers in these cascade structures. Initial attempts to overcome this bottleneck were carried out using a variety of electron acceptors as an alternative to fullerene. However, increasing the Voc was detrimental to the current density, therefore the best OPVs remain those constructed using fullerene.

Keywords: Organic solar cells; energy materials; photovoltaic; semiconductor materials; interface; thin film

***Corresponding authors:** Jean Christian Bernède, Email: jean-christian.bernede@univ-nantes.fr; Present address: FSTN, 2 rue de la Houssinière 44322, Nantes France; Linda Cattin, Email:linda.cattin-guenadez@univ-nantes.fr

1. Introduction

Nowadays, organic photovoltaic solar cells (OPVs) show great potential due to their high efficiency, flexibility, low weight and semi-transparency [1, 2]. The progress in this area of research has been possible due to the exploration of new materials and configurations, which has led to an improvement in various organic photovoltaic solar cell (OPV) parameters; for instance, the use of new organic materials and optimized configurations, such as tandem OPVs [3]. Although it is interesting to develop high-performance products and/or configurations, it is important to keep in mind other important criteria such as the facile synthesis of the requisite organic materials and control over the fabrication process. For instance, ternary structures with a cascade energy alignment allow exciton dissociation and carrier collection without the need of recombination layers, which are necessary in tandem OPVs [4]. On the other hand, charge generation can take place not only at an electron donor/electron acceptor (E_D/E_A) interface, which corresponds to the classical four step process [5], but also via a two-step exciton generation process at the E_D/E_A interface [6], opening up the possibility for three-layer devices. This last process consists of two-steps involving exciton diffusion from the donor to the acceptor over long length scales and dissociation. Diffusion over a long length scale is possible through Förster resonance energy transfer (FRET) [7, 8].

In the present study, we chose to mainly work with commercial molecules in planar heterojunctions (PHJ). This configuration exhibits low performance when compared to bulk heterojunctions (BHJ), but they are easier to implement. If BHJs achieve high efficiency, good performances can also be expected to be obtained using PHJs, as demonstrated in the literature [9–17]. Small molecules present some advantages, such as facile purification and more reproducible synthesis, leading to a unique final product without any batch-to-batch variation [18]. The use of thermal evaporation under vacuum permits facile control over the structural architecture and management of the film morphology using the deposition rate [19] and nature of the substrate [20]. Moreover, deposition via sublimation results in an improvement in the layer purity, leading to highly reproducible device fabrication [21–23]. Therefore, in the present work we have studied OPVs based on small molecules deposited using a vacuum process. In the ternary structure, the central organic layer must be ambipolar (E_{DA}) with sufficient carrier mobility, holes and electrons. Moreover, the use of a ternary PHJ induces an increase in the series resistance of the OPV device, therefore, it is recommended to use organic molecules with good carrier mobility. Boron subphthalocyanine chloride (SubPc), which exhibits a very high absorption coefficient and ambipolar conductivity [24], was chosen as the central layer in our ternary structure. We chose fullerene (C_{60}) as the electron acceptor due to its high electron mobility and very high efficiency toward collecting excited electrons [25]. The third layer, the electron donor, was pentacene due to its high hole mobility [26, 27]. Schematic representations of typical PHJ-OPVs are shown in the supporting information (Fig. S1).

In regard the pentacene layer, it has been shown that the substrate properties significantly influence its properties, such as grain size, and therefore, the carrier diffusion length [28]. In addition, it has been shown that when the grain size is increased, the scattering probability of the charge carriers is decreased due to the reduced grain boundary density, which results in an increase in the maximum drain current observed in thin film transistors [27]. For instance, the

carrier mobility increases by one order of magnitude after annealing due to an increase in the grain size [29]. On the other hand, as shown by Hsiao Wen Zan et al. [30], the grain size in pentacene thin films increases with the surface energy of the substrate.
In the case of OPVs, the under layer of the E_D, in this case pentacene, is a thin layer called the hole extracting layer (HEL), which increases the band matching between the ITO anode and the E_D. Actually, in the case of some phthalocyanine dyes, we have shown that if both MoO_3 and CuI are used as the HEL, the resulting hybrid MoO_3/CuI layer can allow the best OPV efficiency to be achieved [31]. Nevertheless, we have also shown that the surface energy of MoO_3 is significantly higher than that of CuI. Therefore, in the present work, we used MoO_3 as the HEL to optimize the properties of the pentacene layer.
After a systematic characterization of the PHJ-OPVs based on Pentacene/SubPc/C_{60} we widened our study to two others E_As in order to increase the open circuit voltage, which is quite small in the case of the Pentacene/C_{60} couple. These E_As were PCBM (phenyl-C61-butyric acid methyl ester) and EH-IDTBR ($C_{72}H_{88}N_6O_2S_8$) (Figure 1), and the reason for their selection will be discussed below. The chemical structures of the small molecules used in this study are shown in Figure 1.
We named the OPVs based on the three layer structure comprised of Pentacene/SubPc/E_A as "ternary OPVs", while those using a simple couple, *i.e.* Pentacene/SubPc, Pentacene/E_A or SubPc/E_A, were called binary structures (Supporting information S1a and S1b).

2. Experimental

2.1 Organic molecules
The majority of the chemical products used in this study, including pentacene, SubPc, C_{60}, BCP, MoO_3 and Al, were obtained from CODEX-International (France), while PCBM and EH-IDTBR were purchased from Aldrich. Their chemical structures are shown in Figure 1.

2.2 Organic photovoltaic cell deposition process and characterization
The substrate preparation and OPV deposition processes have already been described in the literature [32] and are briefly described in supporting information S2, except for pentacene. In regard pentacene, it has been shown previously that depositing pentacene at a deposition rate of 0.05 nm/s allows the formation of a larger grain size [33, 34]. Schematic representations of the OPVs used in this study are shown in supporting information S1a and S1b, while the characterization techniques are presented in supporting information S3.
In order to obtain a high extraction efficiency for the electrical carriers, hole and electron extracting layers are desirable to improve the power conversion efficiency (η) in the OPVs. Therefore, an exciton blocking layer (EBL) was inserted between the E_A and Al cathode. The EBL was bathocuproine [35]. MoO_3 was used as the HEL inserted between the ITO anode and E_D, as justified above. Some attempts were carried out using a MoO_3/CuI HEL to check the validity of this choice.
Therefore, the organic molecules used in the active layers were pentacene, SubPc, C_{60} and PCBM or EH-IDTBR. Among them, C_{60}, PCBM and EH-IDTBR were the E_A in the ternary OPVs, while due to the fact that it is ambipolar, SubPc was used as the central layer. Finally,

aluminium film was used as the cathode. Regarding the choice of SubPc as the central layer, it was used not only due to the fact that it is ambipolar, but also because it has intermediate HOMO and LUMO values between those of the donor (pentacene) and acceptors. It must be noted that SubPc, which has an electron mobility of 8×10^{-3} $cm^2V^{-1}s^{-1}$, has already been successfully inserted between an E_D and E_A [24, 36].
Therefore, the structures used were as follows:
Glass/ITO (100 nm)/MoO_3 (3 nm)/organic active layers/BCP (9 nm)/Al (120 nm).

3. Results

After an optical and electrical study of the different OPVs, we proceeded to perform some morphological characterization using SEM and AFM in order to help toward understanding the different behaviour observed for the OPVs.

3.1 Optical and electrical (J-V characteristics and external quantum efficiency (EQE)) studies on the OPVs using C_{60} as an electron acceptor.

In parallel to the study of ternary OPVs, we studied binary OPVs constructed from all possible combinations in order to verify if the multiple interfaces within the ternary structure are all active or not. Therefore, we fabricated a set of planar heterojunction OPVs based on the Pentacene/C_{60}, SubPc/C_{60} and Pentacene/SubPc couples as control devices.
The absorption spectra of the different layers used and those of their stacks are represented in Figure 2. The total absorption of the stacked layers corresponds to the sum of the absorption of the three stacked layers.
The typical J-V characteristics observed for these devices are presented in Figure 3, while the results are summarized in Table 1. The results given in Table 1 were obtained after optimisation of the thickness of the different layers constituting the active OPV. These optimisations are reported in supporting information S4.
Firstly, it can be noted that the efficiency of the Pentacene/C_{60} binary OPV was in good agreement with values reported in the literature [33, 37]. Similarly, the SubPc/C_{60}couple gives results in accordance with those previously reported [38, 39]. On the other hand, the performance of the Pentacene/subPc OPV was very poor. However, the ternary OPV allowed a significant increase in the performance since, when compared with the best result obtained for the binary structures (*i.e.*, the SubPc/C_{60} OPV), there was a 10% increase in the efficiency. It must be noted that the ternary structures using MoO_3/CuI as the HEL exhibit lower efficiencies to those obtained using MoO_3. This confirms that our choice of HEL was judicious. In regard the EQE, if we compare the shape of absorption and EQE spectra (Figure 2b and 4) we can see that the EQE spectra reproduce the shape of their corresponding absorption curves. Therefore, the contribution of the three organic molecules to the current generation is clearly visible.
Nevertheless, at first glance, when looking at Figure 3, it is immediately noticeable that the presence of pentacene strongly limits the Voc value.
More precisely, as shown in Table 1, the ternary OPV comprised of Pentacene/SubPc/C_{60} achieved the highest Jsc value. Upon comparison with the binary OPVs constructed using

pentacene as the E_D, the ternary structure showed a significant increase in the OPV performance. Moreover, due to its high Jsc value, the efficiency of the ternary Pentacene/AlPcCl/C_{60} OPV was higher than that of the binary OPV constructed from SubPc/C_{60}, and was also better than the performance observed for the ternary OPV prepared using MoO_3/CuI as the HEL.

In order to check the influence of MoO_3 and CuI on the morphology of the pentacene layers, we carried out SEM and AFM analyses (Figure 5). The SEM images of the surface of the ITO/MoO_3/pentacene (Figure 5c) and ITO/MoO_3/CuI/pentacene (Figure 5d) structures show that the grain size of the pentacene layers deposited onto MoO_3 was higher than that of the thin films deposited onto CuI.

This result was confirmed by AFM analysis. To determine the surface roughness and grain size of the samples, several representative parameters were selected. The surface roughness was investigated using the mean roughness (Ra) and mean square roughness (Rq), while a specific module of Gwyddion software was used to evaluate the particle statistics (grain number, mean grain size and total projected boundary length). It should be stressed here that to mark and quantify particles from the AFM images, the thresholding method was used (Table 2). The AFM images obtained for ITO/MoO_3/pentacene (Figure 5a) and ITO/MoO_3/CuI/pentacene (Figure 5b) confirm the difference in the grain sizes observed during SEM analysis. More precisely, the particle statistics (grains number, mean grain size and total projected boundary length) reported in Table 2 clearly show that the grain size of the pentacene films deposited onto MoO_3 was significantly higher than that of the films deposited onto CuI, and it follows that the grain boundary length decreases. The larger grain size and smaller grain boundary length induces a lower carrier trap density, which results in the higher Jsc value. Moreover, it can be seen in Table 2 that the pentacene films deposited onto MoO_3 are rougher than those deposited onto CuI, which makes the interface area with the top layer larger, which induces a higher charge separation efficiency. All these morphological differences justify that the Jsc value is higher in the OPV constructed using MoO_3 as the HEL.

The EQE measurements are reported in Figure 4 and as-mentioned above, the shape of the curve shows that all the organic layers in the ternary OPVs contribute to the charge carrier generation process. This means that while the very low efficiency observed for the binary Pentacene/SubPc OPV shows that the interface between these two layers is not efficient in terms of charge carrier separation, both layers are active in the ternary structures. It is known that SubPc/C_{60} is an efficient couple in OPVs, which justifies the contribution of SubPc in the EQE curves. In the case of pentacene, the Pentacene/SubPc couple is inefficient as a charge separator and the contribution of pentacene to the EQE spectrum must be attributed to the FRET process. This energy transfer, to be efficient, needs significant overlapping of the E_D emission spectrum with the E_{DA} absorption spectrum [41]. The photoluminescence spectrum of pentacene has already been studied and six photoluminescent bands (A1–A6) were identified [42]. If the main band is situated at λ = 677 nm, the A5 and A6 bands are situated between 520 and 620 nm. Since SubPc absorbs between 500 nm and 650 nm, there is a significant overlap between the photoluminescence of pentacene and the absorbance of SubPc.

3.2 OPVs constructed using electron acceptors others than C_{60}.

Since, as discussed below, the Voc value depends on the energy difference between the energy levels of the highest occupied molecular orbital (HOMO) of the donor and the lowest unoccupied molecular orbital (LUMO) of the acceptor, in order to try to increase the Voc value, we have substituted the C_{60} E_A with smaller absolute LUMO values (Table 3).

One of them is well-known, PCBM, which is used in BHJs in place of C_{60} due to its far higher solubility; the other is EH-IDTBR (Figure 1), which has been recently used with success in a C_{60} free BHJ [44]. The results obtained with these EA's are summarized in Table 4.

As-mentioned above, in order to avoid the Voc limitation induced by the small $\Delta(HOMO_{Pentacene} - LUMO_{C60})$ value, we chose other acceptors which, theoretically, may lead to a higher Voc value (Table 3). If there is an increase in the Voc value, in return, the Jsc value will be reduced, which results in limited efficiency. In the case of EH-IDTBR, if the efficiency of the ternary Pentacene/SubPc/EH-IDTBR OPV was higher than that of the binary OPVs, Pentacene/EH-IDTBR (Table 4) and Pentacene/SubPc (Table 1), it is smaller than that observed for the SubPc/EH-IDTBR OPV. Moreover, the highest efficiency obtained with OPVs prepared using EH-IDTBR was due to the ternary OPV comprised of Pentacene/EH-IDTBR/C_{60}, which shows that, when deposited under vacuum, EH-IDTBR is not as efficient acceptor as C_{60}. The same tendency was observed with PCBM. The efficiency of the ternary structure constructed from Pentacene/SubPc/PCBM was $\eta = 0.50\%$, while that of the binary structure (Pentacene/PCBM) was $\eta = 0.20\%$. If there was a small increase in the Voc value when compared with the OPVs prepared using C_{60} as the E_A, which was expected, and if the FF was acceptable, the Jsc value is very small. Although the deposition of these materials via sublimation under vacuum is not usual, we have attempted to check whether some degradation took place during the deposition process.

In order to check if the deposition of EH-IDTBR under vacuum induced some degradation, we measured its optical density. Its spectrum is shown in Figure 6. By comparison with the absorption of the thin film deposited via spin coating, there was no difference observed in its spectrum [45].

The preservation of EH-IDTBR was also confirmed using XPS analysis. In accordance with the optical study, no difference was observed between the powder and thin film XPS spectra (Figure 7). The small extra peaks visible in the thin film spectrum were attributed to In and Si, due to the EH-IDTBR being deposited on ITO coated glass. It can be concluded that there was no significant degradation of EH-IDTBR during the sublimation step.

In regard the PCBM layer, some studies have already been performed. Hergen Eilers showed using infrared spectroscopy that the main contributions to the infrared spectra of PCBM were preserved after deposition under vacuum with the bands corresponding to the side chains of PCBM being observed [46]. Therefore, EH-IDTBR and PCBM were not significantly damaged during their deposition. All these results are discussed below.

4. Discussion

In OPVs, the energy levels of the HOMO and LUMO of the organic materials are primordial. Not only does the energy difference between the LUMO and HOMO (*i.e.* the band gap) of the organic molecules determine the light absorption, but also the relative energy levels of the LUMO and HOMO of the E_D and E_A are very important. Actually, in order to obtain highly

efficient exciton charge separation, the offset of the LUMOs (HOMOs) values must be greater than the energy of the exciton (ΔE_{exc}). On the other hand, it is now generally accepted that the open circuit voltage of a binary OPVs is as follows (HOMO and LUMO in absolute values) [47, 48]:

$$qVoc = HOMO_{ED} - LUMO_{EA} - X \quad (0.3\ eV < X < 0.6\ eV \text{ in the case of a PHJ}) \quad (1)$$

It is therefore necessary to find the best compromise between the gap value of the E_D, the energy difference between the LUMOs (HOMOs) of E_D and E_A, and the Voc value (Figure 8).

In the case of three stacked layers, in terms of the Voc value, there is some controversy in regard the requirement concerning the band structure of the materials used. In the cascade configuration of the band structure (Figure 9) it is generally thought that it is necessary to use an E_D with a HOMO (or E_A with LUMO) aligned with that of the central layer E_{DA} in order to avoid any reduction in the Voc value. This hypothesis has been supported in the literature, for instance, Cnops et al. confirmed that the Voc value is ultimately limited by the energy levels of the outer layers in the cascade structure [14]. However, this assertion was weighted by other works dedicated to BHJs, where both E_D's were blended. In this case, these OPVs have a tuneable Voc value, which is dependent on the composition of the mixed layer, instead of being restricted to the lowest Voc value dictated by the lower HOMO level. The Voc value observed for the ternary OPVs is an intermediate value between the low and high Voc (Figure 9) [49].
More recently, it has been shown that planar OPVs prepared with a four layer cascade architecture exhibit a Voc value that is greater than the offset in energy between the HOMO of the outmost E_D and the LUMO of the outmost E_A (Low Voc in Figure 3) [50]. In fact, as shown in Table 1, the Voc value does not surpass 0.46 eV, which confirms that the Voc value is limited by the offset in energy between the HOMO of the outmost E_D and the LUMO of the outmost E_A (Low Voc in Figure 9).
SubPc has already been used as an ambipolar layer in ternary PHJ-OPVs [24, 51], however, in this work, the properties of the E_D were different from those of pentacene. For instance, in Ref. 51, the hole mobility of the E_D was small, while in the present work, the hole mobility of pentacene is high. More importantly, the electron donor and the central ambipolar layers have the same HOMO value, therefore there is no need to discuss the Voc value (high Voc-low Voc) [51], while it is a major contribution in the present study. Consequently, the objective in the present work is not achieving very high efficiency, but to contribute to the current debate surrounding the Voc value. The different LUMOs and HOMOs absolute values of the organic molecules used during this work are given in Table 1. It can be deduced from formula (1) that the maximum theoretical Voc value of the ternary PHJ Pentacene/SubPc/C_{60} OPV was only 0.6 eV with the HOMO value of pentacene being 4.9 eV. Therefore, beyond an exhaustive study of ternary Pentacene/SubPc/C_{60} OPVs, we performed an extensive study of the ternary OPVs using an E_A with LUMO values expected to give high Voc values (Table 1).
Actually, the maximum theoretical Voc values associated with PCBM are: "low" Voc = 1.2 V and "high" Voc = 1.9 V, and "low" Voc = 1 V and "high" Voc = 1.7 V with EH-IDTBR (Figure 3 and Table 1). A comparison of the results presented in Tables 2 and 3 shows that

there is indeed an increase in the Voc value. Nevertheless, the Voc increase is far from its maximum theoretical value and corresponds clearly to the "low" Voc value, which confirms that the Voc value is limited by the offset in energy between HOMO of the outmost E_D and the LUMO of the outmost E_A (Low Voc in Figure 9).

Nevertheless, given the small Voc value, interesting OPV efficiencies were achieved when using MoO_3 as the HTL due to the improved morphology of pentacene when deposited onto MoO_3. The influence of the ITO/MoO_3 anode on the OPV properties using pentacene as the E_D has already been discussed upon comparison with bare ITO [40]. In the present work we have shown that the as-obtained performance was not as good as those obtained with MoO_3, even when a CuI HTL was deposited onto ITO (Table1). As evocated in the previous paragraph, the high Jsc value was not only due to MoO_3, but also to the occurrence of FRET. As a matter of fact, our experimental EQE spectra demonstrate that the very low efficiency of the binary Pentacene/SubPc OPV shows that the interface between these two layers is not efficient in terms of the charge carrier separation, but both these layers are active in the ternary structures. Firstly, the different behaviours of the interfaces observed in the Pentacene/SubPc (inefficient, *i.e.* unfavourable configuration) and Pentacene/C_{60} (efficient, *i.e.* favourable configuration) couples are a good illustration of the theoretical work of Ryno et al. [52]. Actually, these authors have shown that if the charge separation in the planar configuration is not easy due to the presence of a barrier to charge separation, there are several effects that will act to reduce or negate this large barrier. They have shown that such positive effects are present at the Pentacene/C_{60} interface. In the present work, if we confirm the high efficiency of charge separation at this interface, we can show that this is not the case for the Pentacene/SubPc interface, even if they both have a favourable cascade energy alignment.

In regard the FRET process, it is well documented in review papers such as those of Stoltzfus et al. [**7**] and An et al. [8] that it is possible between pentacene and SubPc, which justifies the pentacene contribution to the EQE spectrum. This contribution via FRET to the charge collection results in the enhanced Jsc and η values. This alternative migration route for excitons created in the E_D is decisive toward obtaining improved ternary OPVs when compared to their corresponding binaries.

As-mentioned above, the sensitization of pentacene to SubPc was asserted from Figure 4. An EQE contribution between 625 and 700 nm corresponding to the main absorption peak of pentacene is clearly visible. This behaviour suggests that the pentacene excitons produced via optical absorption are transferred to the SubPc layer, since, as shown by the poor behaviour of the Pentacene/SubPc OPV, the Pentacene/SubPc interface is inefficient in separating the exciton charges. Such FRET has already been confirmed in other ternary PHJ-OPVs, such as a-6T/SubNc/SubPc [14]. This example is not isolated, for instance, it has been shown that the planar multi-heterojunction comprised of (thiophene/phenylene)co-oligomers/metal-phthalocyanine/fullerene results in an improved short circuit current via efficient FRET [53]. Moreover, not only has the efficient energy transfer from pentacene to PbSe nanocrystals been reported [54], but also that observed between pentacene and ZnPc, a phthalocyanine dye similar to SubPc [55]. All these findings confirm the presence of the FRET process.

A relatively high Jsc value was obtained, although the carrier mobility of the organic materials used is quite different. Actually, even without any annealing, the hole mobility (μ_h) in pentacene was 0.1 $cm^2\ V^{-1}\ s^{-1}$ [26, 27], which is higher than the carriers mobility in SubPc ($\mu_h = 1.69\times10^{-5}\ cm^2\ V^{-1}\ s^{-1}$), while the electron mobility (μ_e) was $8\times10^{-3}\ cm^2V^{-1}s^{-1}$ [51]. Nevertheless, the electron mobility of C_{60} was of the same order of magnitude as the hole mobility of pentacene. In C_{60}, the μ_e value is $0.5–2\times10^{-1}cm^2V^{-1}s^{-1}$ [56, 57]. Tress et al. [58] have shown that, in the case of a planar binary OPV, an imbalanced mobility ratio of nearly 100 is acceptable and that, in any case, regarding the OPV performance, imbalanced high/low mobilities are preferable when compared to balanced low mobilities. Moreover they have shown that a very high imbalanced mobility ratio induces S-shaped J-V characteristics. In the case of our ternary PHJ-OPVs, there was no S-shaped tendency, which confirmed that the difference in carrier mobility between pentacene and SubPc was not fatal, even if the decrease in the FF value of the pentacene/SubPc/C_{60} OPV relative to that obtained for the Pentacene/C_{60} OPV was probably due to this mobility difference.

Nevertheless, if these ternary OPVs exhibit high Jsc values, their efficiency is limited by their small Voc values due to the small $HOMO_{ED}$-$LUMO_{EA}$ value. Therefore, we used E_D/E_A pairs with larger $HOMO_{ED}$-$LUMO_{EA}$ values to try to increase the Voc value of the OPVs, the new E_As chosen were PCBM and EH-HIDTBR (Figure 1). The two OPVs prepared using these E_As have a classical cascade band structure with significant LUMO and HOMO offsets (Table 3), however, the results shown in Table 4 were quite disappointing. In fact, the obtained efficiencies were smaller than those obtained with C_{60}, even though the EH-IDTBR and PCBM molecules were not significantly damaged during their deposition. This is probably due to the fact that when used in the PHJ with a corresponding high E_A film thickness, their conductivity is small and the morphology of these films was not optimized as in the case of the BHJ. Nevertheless, the increase in the Voc value obtained is promising and will encourage future efforts to improve the morphology of the multilayer device.

Conclusions

In the present work, we have extensively studied the Pentacene/SubPc/C_{60} cascade PHJ for the first time, which showed systematically that the measured Voc values are smaller than the offset in energy between the HOMO of the outmost E_D and the LUMO of the outmost E_A. Therefore, the Voc value is limited by the "low Voc" (Figure 3). However, we have shown that ternary OPVs prepared using the Pentacene/SubPc/C_{60} active structure result in improved cell performance when compared with those obtained with their corresponding binary structures via an improvement in the Jsc. The increase in the Jsc value is attributed to the presence of FRET. Nevertheless, this improvement is limited by the Voc value. Our first attempts using a more favourable band structure, *i.e.* an E_A with smaller LUMO value, to increase the Voc value failed to increase the OPV efficiency due to the limited Jsc values. However, recent studies have shown that many new molecules behave as effective acceptors, which may be successfully used in ternary OPVs with pentacene as the E_D.

Acknowledgments: The authors acknowledge the funding received from the CNRST (PPR/2015/9) Ministère, Morocco).

References

[1] Z. Hu, L. Ying, F. Huang, Y. Cao, Towards a bright future: polymer solar cells with power conversion efficiencies over 10%, Sci. Chin. Chem. 60 (2017) 571–582. doi: 10.1007/s11426-016-0424-9

[2] X. Ma, W. Gao, J. Yu, Q. An, M. Zhang, Z. Hu, J. Wang, W. Tang, C. Yang, F. Zhang F, Ternary non-fullerene polymer solar cells with efficiency >13.7% by integrating the advantages of the materials and two binary cells, Energy Environ. Sci. 8(2018) 2134–2141. doi: 10.1039/c8ee01107a

[3] X. Che, Y. Li, S. R. Forrest, High fabrication yield organic tandem photovoltaics combining vacuum and solution processed subcells with 15% efficiency, Nat. Energy.3 (2018) 422–427. doi: 10.1038/s41560-18-0134-z

[4] A. P. Yuen, A-M. Hor, J. S. Preston, R. Kienkler, N. M. Bamsey, R. O. Loutfy, A simple parallel tandem organic solar cell based on metallophthalocyanines, Appl. Phys. Lett. 98 (2011) 173301. doi: 10.1063/1.3579250

[5] P. Peumans, S. R. Forrest, Separation of geminate charge-pairs at donor-acceptor interfaces in disordered solids, Chem. Phys. Lett. 398 (2004)27–31.doi: 10.1016/j.cplett.2004.09.030

[6] D. C. Coffey, A. J. Ferguson, N. Kopidakis, G. Rumbles, Photovoltaic charge generation in organic semiconductors based on long-range energy transfer, ACSNano. 4 (2010) 5437–5445. doi: 10.1021/nn101106b

[7] D. M. Stoltzfus, J. E. Donaghey, A. Armin, P. E. Shaw, P. L. Burn, P. Meredith, Charge generation pathways in organic solar cells: Assessing the contribution from the electron acceptor, Chem. Rev. 116 (2016) 12920–12955. doi:10.1021/acs.chemrev.6b00126

[8] Q. An, F. Zhang, J. Zhang, W. Tang, Z. Deng, B. Hu, Versatile ternary organic solar cells: A critical review, Energy Environ. Sci. 9 (2016) 281–322. doi:10.1039/C5EE02641E

[9] S. Sista, Y. Yao, Y. Yang, M. L. Tang, Z. Bao, Enhancement in open circuit voltage through a cascade-type energy band structure, Appl. Phys. Lett. 91 (2007) 223508. doi: 10.1063/1.2817935

[10] T. D. Heidel, D. Hochbaum, J. M. Sussman, V. Songh, M. E. Bahlke, I. Hiromi, J. Lee, M. A. Baldo, Reducing recombination losses in planar organic photovoltaic cells using multiple step charge separation, J. App. Phys. 109 (2011) 104502. doi: 10.1063/1.2817935

[11] C. W. Schlenker, V. S. Barlier, S. W. Chin, M. T. Whited, R. E. McAnally, S. R. Forrest, M. E. Thompson, Cascade organic solar cells, Chem. Mater. 23 (2011) 4132–4140. doi: 10.1021/cm200525h

[12] K. Cnops, B. P. Rand, D. Cheyns, P. Heremans, Enhanced photocurrent and open-circuit voltage in a 3-layer cascade organic solar cell. Appl. Phys. Lett. 101 (2012) 143301. doi: 10.1063/1.4757575

[13] B. Vereet, K. Cnops, D. Cheyns, P. Heremans, A. Stesmans, G. Zango, C. G. Claessens, T. Torres, B. P. Rand, Decreased recombination through the use of a non-fullerene acceptor in a 6.4% efficient organic planar heterojunction solar cell, Adv. Energy Mater. 4 (2014) 1301413. doi:10.1002/aenm.201301413

[14] K. Cnops, B. P. Rand, D. Cheyns, B. Verreet, M. A. Empl, P. Heremans, 8.4% efficient fullerene-free organic solar cells exploiting long-range exciton energy transfer, Nat. Commun. 5 (2014) 3406.doi: 10.1038/ncomms4406

[15] A. Barito, M. E. Sykes, B. Huang, D. Bilby, B. Frieberg, J. Kim, P. F. Green, M. Shtein, Universal design principles for cascade heterojunction solar cells with high fill factors and internal quantum efficiencies approaching 100%, Adv. Energy Mater. 4 (2014) 1400216–??. doi: 10.1002/aenm.201400216
[16] M. A. Stevens, A. C. Arango, Open-Circuit voltage exceeding the outmost HOMO-LUMO offset in cascade organic solar cells, Org.Electron.37 (2016) 80–84. doi: 10.1016/j.orgel.2016.06.008
[17] Y. H. L. Lin, M. Koch, A. N. Brigeman, D. M. E. Freeman, L. Zhao, H. Bronstein, N. C. Giebink, G. D. Scholes, B. P. Rand, Enhanced sub-bandgap efficiency of a solid-state organic intermediate band solar cell using triplet-triplet annihilation, Energy Environ. Sci. 10 (2017) 1465–1475. doi: 10.1039/C6EE03702J
[18] A. Leliège, J. Grolleau, M. Allain, P. Blanchard, D. Demeter, T. Rousseau, J. Roncali, Small D-p-A systems with s-phenylene-bridged accepting units as active materials for organic photovoltaics, Chem. Eur. J. 19 (2013) 9948–9960. doi: 10.1002/chem.201301054
[19] Z. El Jouad, L.Barkat, N.Stephant, L.Cattin, N.Hamzaoui, A.Khelil, M.Ghamnia, M. Addou, M.Morsli, S.Béchu, C.Cabanetos, M.Richard-Plouet, P.Blanchard, J.C. Bernède, Ca/Alq_3 hybrid cathode buffer layer for the optimization of organic solar cells based on a planar heterojunction, J. Phys.Chem. Solids. 98 (2016) 128–135. doi: 10.1016/j.jpcs.2016.06.014
[20] M. Makha, L. Cattin, Y. Lare, L. Barkat, M. Morsli, M. Addou, A. Khelil,J. C. Bernède, MoO_3/Ag/MoO_3 anode in organic photovoltaic cells: Influence of the presence of a CuI buffer layer between the anode and the electron donor, Appl. Phys. Lett. 101 (2012) 233307. doi: 10.1063/1.4769808
[21] F. H. Scholes, T. Ehlig, M. James, K. H. Lee, N. Duffy, A. D. Scully, T. B. Singh, K. N. Winzenberg, K. Kemppinen, S. E. Watkins, Intra phase microstructure-understanding the impact on organic solar cell performance, Adv. Funct. Mater.23 (2013) 5655–5663.doi: 10.1002/adfm.201300726.
[22] S. Galindo, M. Ahmadpour, L. G. Gerling, A. Marsal, C. Voz, R. Alcubilla, J. Puigdollers, Influence of the density of states on the open-circuit voltage in small-molecule solar cells, Org. Electron. 15 (2014) 2553–2560. doi:10.1016/j.orgel.2014.07.011
[23] Y-J. Chang, J-L. Hsu, Y-H. Li, S. Biring, T-H. Yeh, J-Y. Guo, S-W. Liu, Carbazole based small molecules for vacuum deposited organic photovoltaic devices with open-circuit voltage exceeding1 V, Org. Electron. 47 (2017) 162–173. doi: 10.1016/j.orgel.2017.05.007
[24] B. Ebenhoch, N. B. A. Prasetya, V. M. Rotello, G. Cooke, Solution-processed boron subphthalocyanine derivatives as acceptors for organic bulk-heterojunction solar cells. J. Mater. Chem. A. 3 (2015) 7345–7352. doi: 10.1039/C5TA00715A
[25] N. S. Sariciftci, L. Smilowitz, A. J. Heeger, F. Wudl, Photoinduced electron transfer from a conducting polymer to buckminsterfullerene, Science, 258 (1992) 1474–1476. doi: 10.1126/science.258.5087.1474
[26] D. J. Gundlach, Y. Y. Lin, T. N. Jackson, S. F. Nelson, D. G. Schlom, Pentacene Organic thin-film transistors-molecular ordering and mobility, IEEE Electron Device Lett. 18 (1997) 87–89. doi: 10.1109/55.556089

[27] S. J. Kang, M. Noh, D. S. Park, H. J. Kim, C. N. Whang, Influence of post-annealing on polycrystalline pentacene thin film transistor, J. Appl. Phys. 95 (2004) 2293–2296. doi: 10.1063/1.1643189
[28] J. Puigdollers, C. Voz, I. Martin, A. Orpella, M. Vetter, R. Alcubilla, Pentacene thin-film transistors on polymeric gate dielectric: Device fabrication and electrical characterization, J. Non-Cryst. Solids.338 (2004) 617–621. doi: 10.1016/j.jnoncrysol.2004.03.054
[29] K-J. Kim, H. Yoo, S-W. Jeong, Y. Roh, Influence of post-deposition annealing of PVP/pentacene films on characteristics of organic thin film transistors, Phys. Status SolidiA. 207 (2010) 1760–1764. doi: 10.1002/pssa.200983741
[30] H. W. Zan, C-W. Chou, K-H. Yen, Surface energy and adhesion energy of solution-based patterning in organic thin film transistors, Thin Solid Films. 516 (2008) 2231–2236. doi: 10.1016/j.tsf.2007.08.003
[31] L. Cattin, J. C. Bernède, Y. Lare, S. Dabos-Seignon, N. Stephant, M. Morsli, P. P. Zamora, F. R. Diaz, M. A. del Valle, Improved performance of organic solar cells by growth optimization of MoO_3/CuI double-anode buffer, Phys. Status Solidi A.210,(2013) 802–808. doi: 10.1002/pssa.201228665
[32] L. Cattin, M. Morsli, J. C. Bernède, Improvement in the lifetime of planar organic photovoltaic cells through the introduction of MoO_3 into their cathode buffer layers, Electronics 3 (2014) 122–131, doi:10.3390/electronics3010122
[33] J. Yang, T-Q. Nguyen, Effects of thin film processing on pentacene/C60 bilayer solar cell performance, Org. Electron. 8 (2007) 566–574. doi: 10.1016/j.orgel.2007.04.005
[34] S. Karak, V. S. Reddy, S. K. Ray, A. Dhar, Organic photovoltaic devices based on pentacene/N, N′-dioctyl-3,4,9,10-perylenedicarboximide heterojunctions, Org. Electron. 10 (2009) 1006–1010. doi: 10.1016/j.orgel.2009.04.006
[35] P. Peumans, S. R. Forrest, Very-high-efficiency double-heterostructure copper phthalocyanine/C_{60} photovoltaic cells, Appl. Phys. Lett. 79 (2001) 126. doi.org/10.1063/1.1384001.
[36] N. Beaumont, S. W. Cho, P. Sullivan, D. Newby, K. E. Smith, T. S. Jones, Boron subphthalocyanine chloride as an electron acceptor for high-voltage fullerene-free organic Photovoltaics, Adv. Funct. Mater. 22 (2012) 561–566. doi: 10.1002/adfm.201101782
[37] W. J. Potscavage, S. Yoo, B. Domercq, B. Kippelen, Encapsulation of pentacene/C_{60} organic solar cells with Al_2O_3 deposited by atomic layer deposition, Appl. Phys. Lett. 90 (2007) 253511. doi: 10.1063/1.2751108
[38] a) J. Kim, S. Yim, Influence of surface morphology evolution of SubPc layers on the performance of SubPc/C_{60} organic photovoltaic cells, Appl. Phys. Lett. 99 (2011) 193303. doi: 10.1063/1.3660710; b) J. Y. Kim, J. Kwak, S. Noh, C. Lee, Enhanced performance of SubPc/C_{60} solar cells by annealing and modifying surface morphology, J. Nanosci. Nanotechnol. 12 (2012) 5724–5727. doi:10.1166/jnn.2012.6414
[39] Y-Q. Zheng, J-H. Zhang, B. Wei, Photocurrent enhancement via structural templating of phthalocyanine based planar heterojunction photovoltaic by a thin layer of dinaphthothienothiophene (DNTT) or 3,4,9,19-perylenetetracarboxylic-dianhydride (PTCDA), Phys. Status Solidi A.212 (2015) 364–368. doi: 10.1002/pssa.201431599
[40] I. Hancox, P. Sullivan, K. V. Chauhan, N. Beaumont, L. A. Rochford, R. A. Hatton, T. S. Jones, The effect of a MoO_x hole-extracting layer on the performance of organic photovoltaic

cells based on small molecule planar heterojunctions, Org. Electron. 11 (2010) 2019–2025. doi: 10.1016/j.orgel.2010.09.014
[41] D. C. Coffey, A. J. Ferguson, N. Kopidakis, G. Rumbles, Photovoltaic charge generation in organic semiconductors based on long-range energy transfer. ACSNano. 4 (2010) 5437–5445. doi: 10.1021/nn101106b
[42] F. Anger, J. O. Osso, U. Heinemeyer, K. Broch, R. Scholtz, A. Gerlach, F. Schreiber, Photoluminescence spectroscopy of pure pentacene, perfluoropentacene, and mixed thin films, J. Chem. Phys. 136 (2012) 054701. doi: 10.1063/1.3677839.
[43] X. Huang, L. Lv, Y. Hu, Z. Lou, Y. Hou, F. Teng, Enhanced performance in inverted polymer solar cells employing microwave-annealed sol-gel as electron transport layers, Org. Electron.42 (2017)107–114. doi: 10.1016/j.orgel.2016.12.031
[44] V. Sharapov, Q. Wu, A. Neshchadin, D. Zhao, Z. Cai, W. Chen, L. Yu, High performance ternary organic solar cells due to favoured interfacial connection by a non-fullerene electron acceptor with cross-like molecular geometry, J. Phys. Chem. C. 122 (2018) 11305–11311. doi: 10.1021/acs.jpcc.8b03013
[45] S. Holliday, R. S. Ashraf, A. Wadsworth, D. Baran, S. A. Yousaf, C. B. Nielsen, C-H. Tan, S. D. Dimitrov, Z. Shang, N. Gasparini, M. Alamoudi, F. Laquai, C. J. Brabec, A. Salleo, J. R. Durrant, I. McCulloch, High-efficiency and air-stable P3HT-based polymer solar cells with new non-fullerene acceptor, Nat. Commun. 7 (2016) 11585. doi: 10.1038/ncomms11585.
[46] H. Eilers, Multispectral visible/infrared sensors based on polymer-metal nanocomposites, Final Progress Report W911NF-06-1-0295 (2010) (https://www.researchgate.net/publication/235023354_Multispectral_VisibleInfrared_Sensors_Based_on_Polymer-Metal_Nanocomposites[47] R. Pode, On the problem of open circuit voltage in metal phthalocyanine/C60 organic solar cells, Adv. Mat. Lett. 2 (2011) 8–11. doi: 10.5185/amlett.2010.12186
[48] J. Benduhn, K. Tvingstedt, F. Piersimoni, S. Ullbrich, Y. Fan, M. Tropiano, K. A. McGarry, O. Zeika, M. K. Riede, C. J. Douglas, S. Barlow, S. R. Marder, Intrinsic non-radiative voltage losses in fullerene-based organic solar cells. Nat. Energy. 2 (2017) 17053. doi: 10.1038/nenergy.2017.53
[49] G. Williams, H. Aziz, Vacuum deposited ternary mixture organic solar cells, Org.Electron.17 (2015) 229–239. doi: 10.1021/acsami.5b09620
[50] M. A. Stevens, A. C. Arango, Open-circuit voltage exceeding the outmost HOMO-LUMO offset in cascade organic solar cells, Org. Electron. 37 (2016) 80–84. doi: 10.1016/j.orgel.2016.06.008
[51] L. Cattin, Z. El Jouad, L. Arzel, G. Neculqueo, M. Morsli, F. Martinez, M. Addou, J. C. Bernède, Comparison of performances of three active layers cascade OPVCs with those obtained from corresponding bi-layers, Sol Energy. 171 (2018) 621–628. doi: 10.1021/jacs.6b01744
[52] S. M. Ryno, Y-T. Fu, C. Risko,J-L; Brédas, Polarization energies at organic-organic interfaces: Impact on the charge separation barrier at donor-acceptor interfaces in organic solar cells, ACS Appl. Mater. Interfaces 8 (2016) 15524–15534. doi: 10.1021/acsami.6b02851

[53] M. Ichikawa. E. Suto, H-G. Jeon, Y. Taniguchi, Sensitization of organic photovoltaic cells based on interlayer excitation energy transfer, Org. Electron. 11 (2010) 700–704. doi: 10.1016/j.orgel.2009.12.023
[54] M. Tabachnyk, B. Ehrler, S. Gélinas, M. L. Böhm, B. J. Walker, K. P. Musselman, N. C. Greenham, R. H. Friend, A. Rao, Resonant energy transfer of triplet excitons from pentacene to PbSe nanocrystals, Nat. Mater. 13 (2014) 1033–1038.doi: 10.1038/nmat4093
[55] Z. R. Hong, R. Lessmann, B. Maennig, Q. Huang, K. Harada, M. Riede, K. Leo, Antenna effects and improved efficiency in multiple heterojunction photovoltaic cells based on pentacene, zinc phthalocyanine and C_{60}, J. Appl. Phys. 106 (2009) 064511. doi: 10.1063/1.3187904
[56] T. D. Anthopoulos, B. Singh, N. Marjanovic, N. S. Saricitci, A. M. Ramil, H. Sitter, M. Cölle, D. M. de Leeuw, High performance n-channel organic field-effect transistors and ring oscillators based on C60 fullerene films, Appl. Phys. Lett. 89 (2006) 213504. doi: doi.org/10.1063/1.2387892
[57] B. P. Rand, J. Gence, P. Heremaans, J. Poortmans, Solar cells utilizing small molecular weight organic semiconductors, Prog. Photovoltaics. 15 (2007) 659–676. doi: 10.1002/pip.788
[58] W. Tress, A. Petrich, M. Hummert, M. Hein, K. Leo, M. Riede, Imbalanced mobilities causing S-shaped IV curves in planar heterojunction organic solar cells, Appl. Phys. Lett. 98 (2011) 063301. doi:10.1063/1.3553764

Figures

Figure 1: The chemical structures of the small molecules investigated in this research study.

Figure 2: (a) The optical density of Pentacene (60 nm)/AlPcCl (15 nm)/C_{60} (40 nm) and the individual Pentacene, SubPc and C_{6O} layers. (b) The OD and EQE spectra of the ternary structure.

Figure 3: The typical J-V characteristics observed for the OPVs based on (♦) Pentacene/C_{60}, (■) SubPc/C_{60}, (●) Pentacene/SubPc and (▲) Pentacene/SubPc/C60 (the filled symbol denotes dark conditions; the empty symbol denotes light-AM1.5- conditions).

Figure 4: The EQE spectra recorded for (■) SubPc/C_{60}, (●) Pentacene/C_{60} and (▲) Pentacene/SubPc/C_{60}.

Figure 5: AFM images of the pentacene layer deposited onto (a) ITO/MoO_3 and (b) ITO/MoO_3/CuI.SEM images of the pentacene layer deposited onto (c) ITO/MoO_3 and (d) ITO/MoO_3/CuI.

Figure 6: The optical density spectrum recorded for a thin film comprised of EH-IDTBR film deposited via sublimation under vacuum.

Figure 7: The XPS spectra recorded for thin film and powdered EH-IDTBR.

Figure 8: A schematic representation of the band structure of a contact E_D/E_A device.

Figure 9: The band structure of the organic materials in aternary OPVs using Pentacene/SubPc/C_{60}as anexample.

Tables

Table 1: A summary of the parameters of the ternary OPV (Pentacene/SubPc/C_{60}) and its corresponding binary structures (* the HTL of this OPV is MoO_3/CuI, while it is MoO_3 for all the other OPVs presented in this table).

Table 2: Grain analysis and surface roughness parameters obtained for the different samples studied. Each analysis was performed from AFM images over a 5µm × 5µm area. The original data was plane-levelled to remove tilt by applying a numerical second-order correction. Particle analysis was carried out using the thresholding method (Gwyddion software).

Table 3: The LUMO and HOMO values of the different electron acceptors studied.
*[42] and **[43].

Table 4: A summary of the parameters of the OPV prepared using the new E_A and its corresponding binary structures

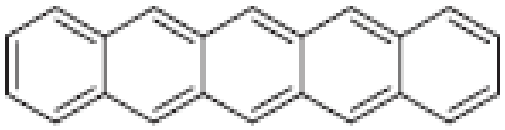

Pentacene

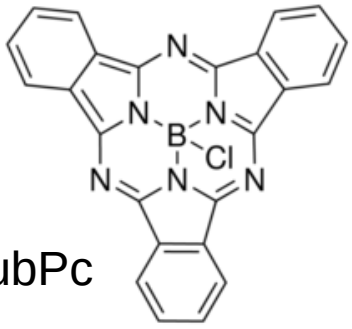

SubPc

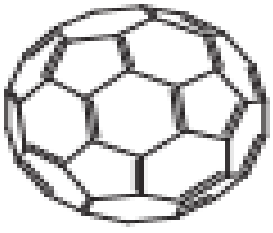

C60

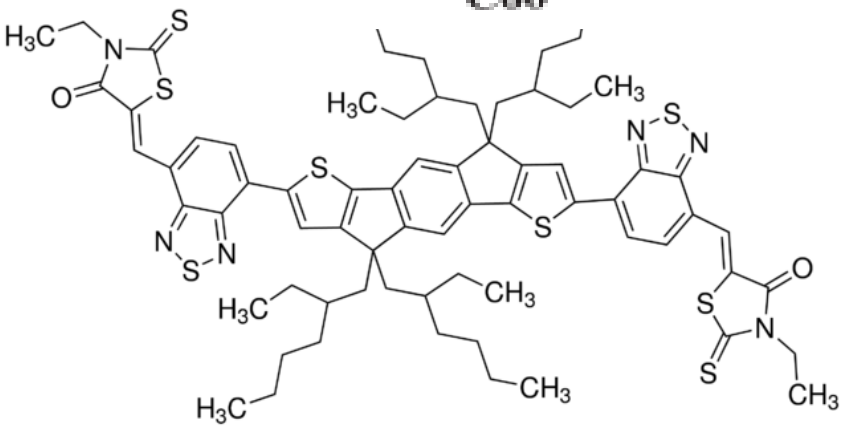

EH-IDTBR

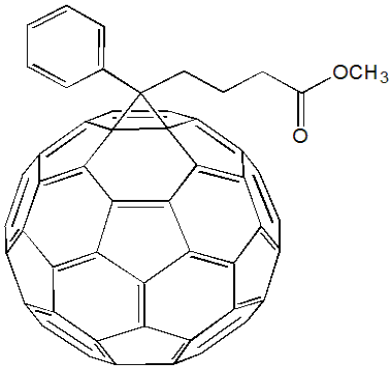

PCBM

Figure 1: The chemical structures of the small molecules investigated in this research study.

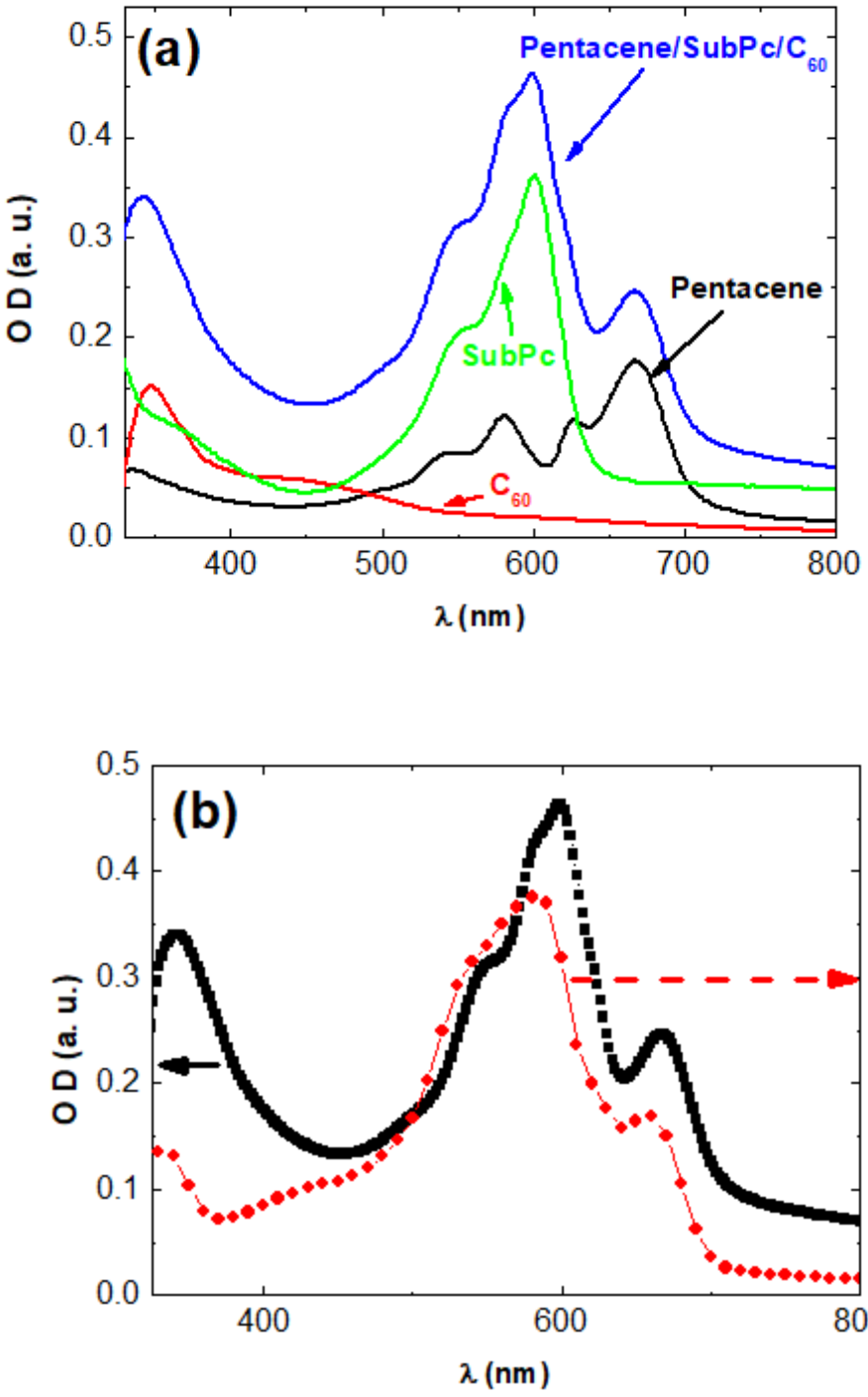

Figure 2:
(a) The optical density of
Pentacene (60 nm)/AlPcCl (15 nm)/C_{60} (40 nm) and the individual Pentacene, SubPc and C_{6O} layers.
(b) The OD and EQE spectra of the ternary structure.

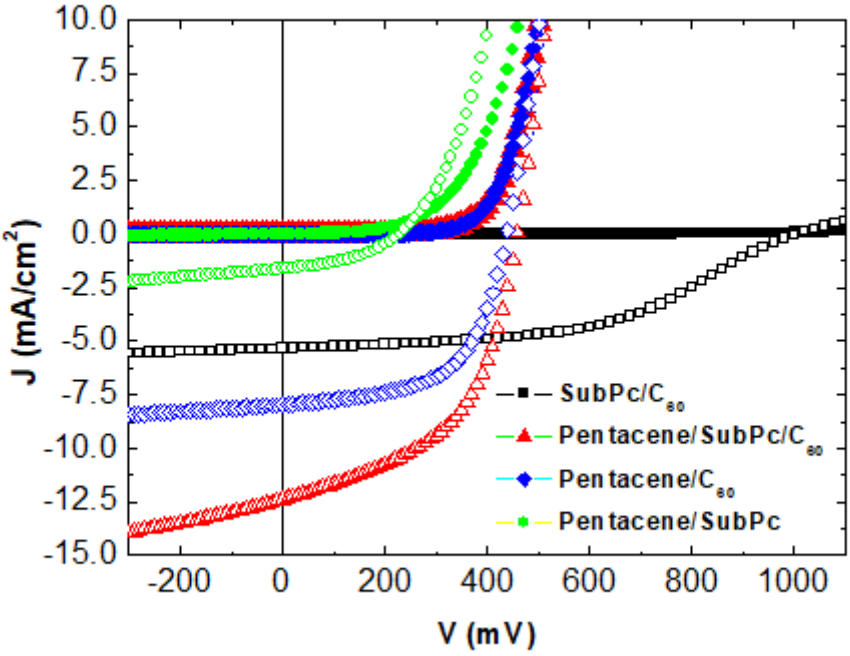

Figure 3: The typical J-V characteristics observed for the OPVs based on (♦) Pentacene/C_{60}, (■) SubPc/C_{60}, (●) Pentacene/SubPc and (▲) Pentacene/SubPc/C60 (the filled symbol denotes dark conditions; the empty symbol denotes light-AM1.5- conditions).

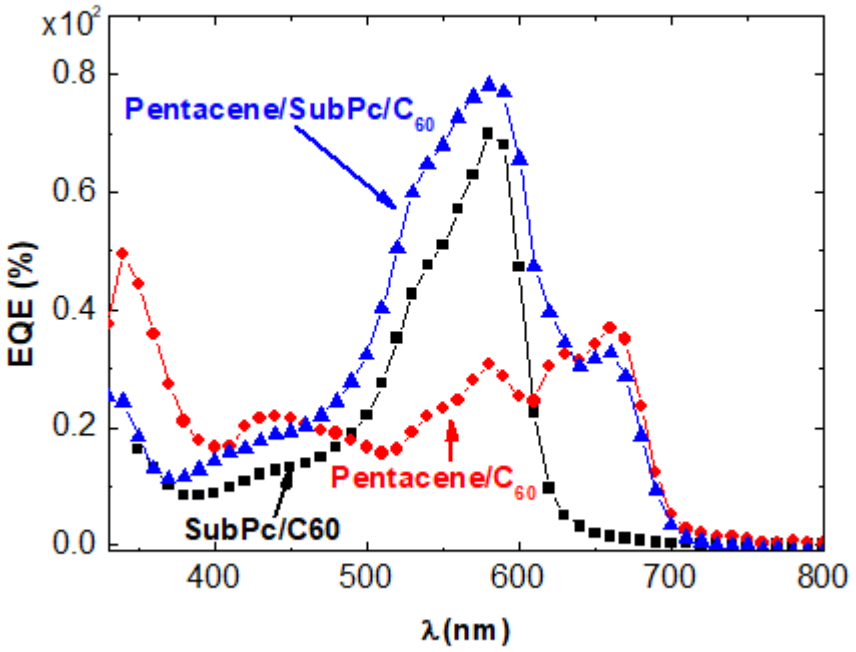

Figure 4: The EQE spectra recorded for (■) SubPc/C_{60}, (●) Pentacene/C_{60} and (▲) Pentacene/SubPc/C_{60}.

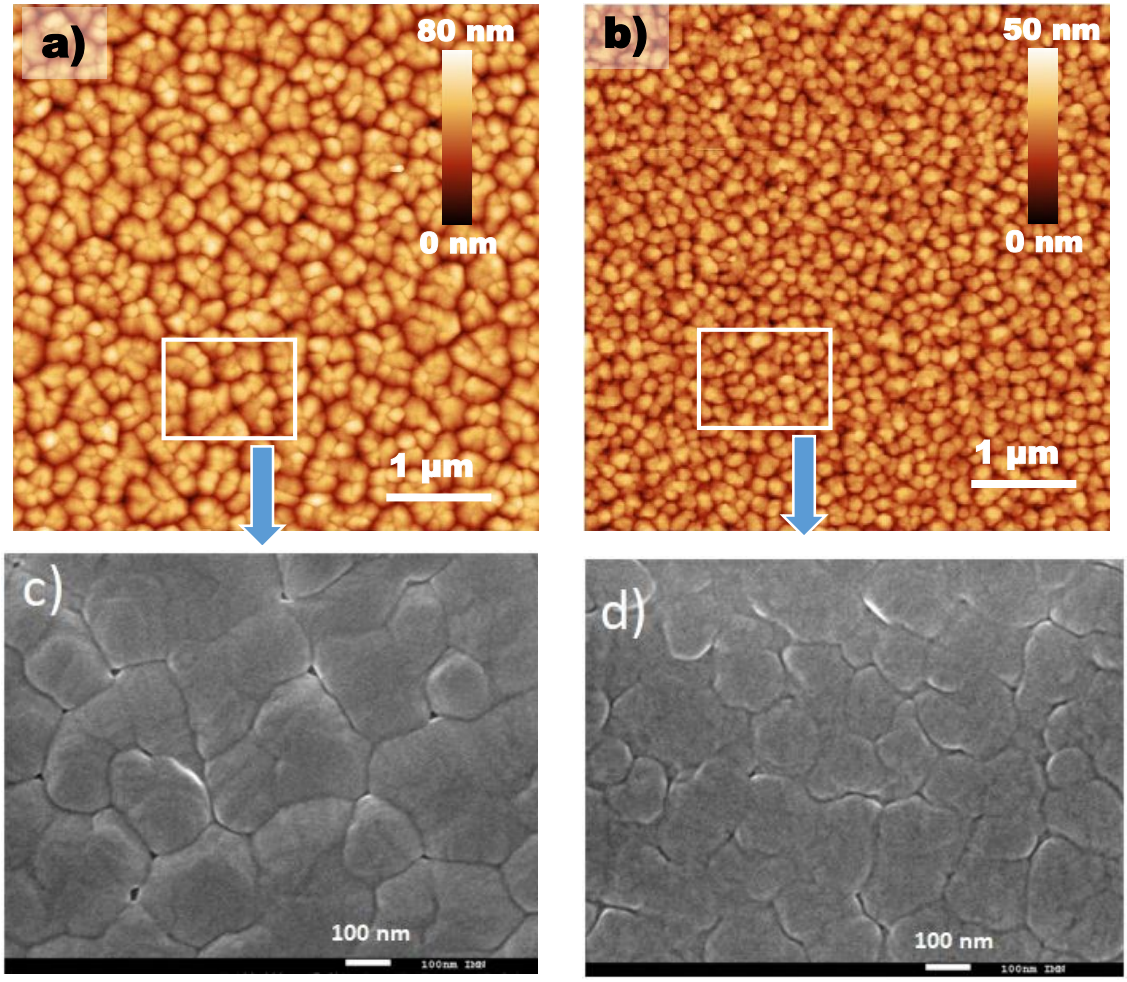

Figure 5: -AFM images of the pentacene layer deposited onto (a) ITO/MoO_3 and (b) ITO/MoO_3/CuI.
-SEM images of the pentacene layer deposited onto (c) ITO/MoO_3 and (d) ITO/MoO_3/CuI.

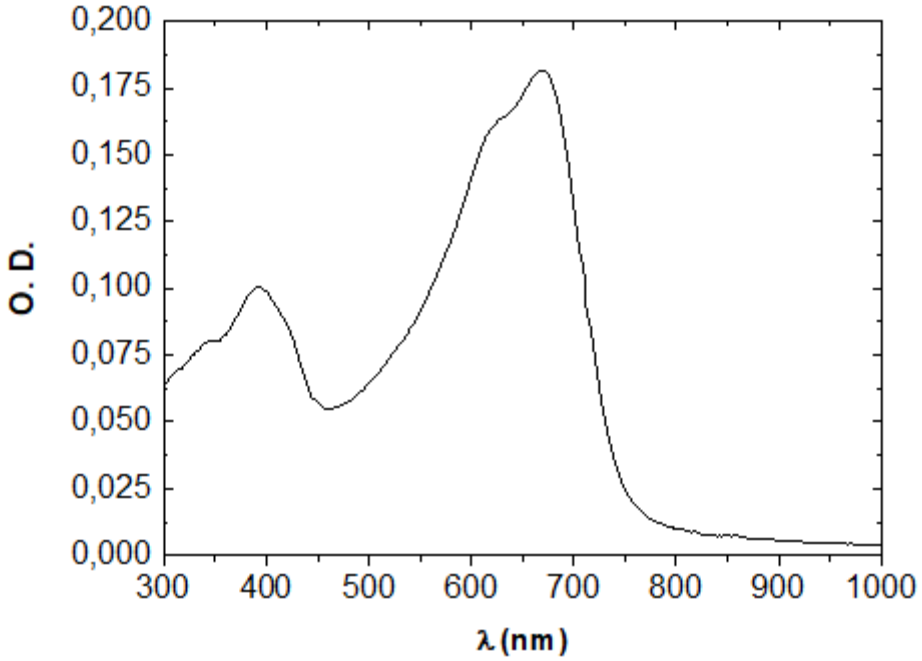

Figure 6: The optical density spectrum recorded for a thin film comprised of EH-IDTBR film deposited via sublimation under vacuum.

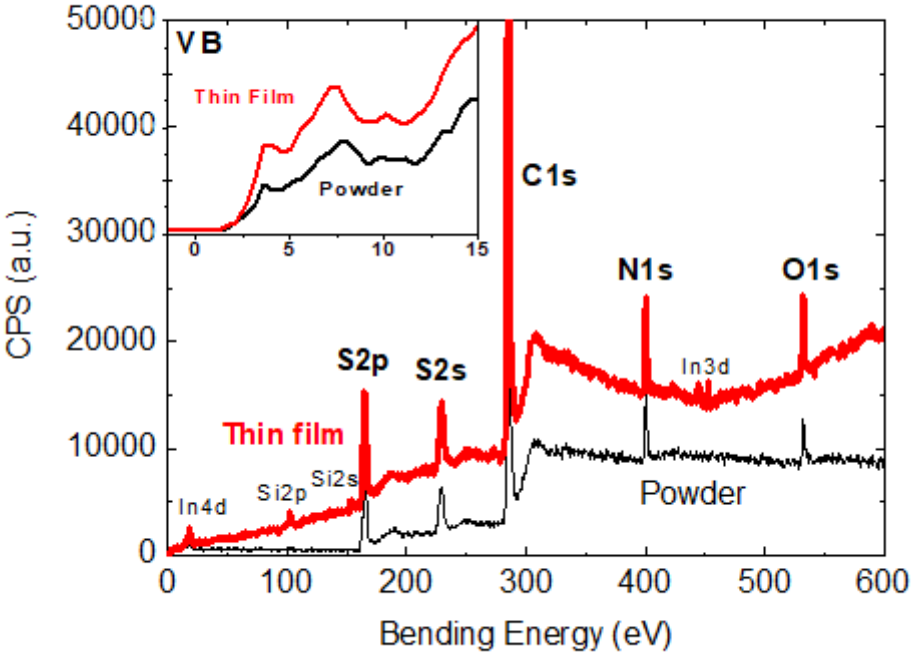

Figure 7: The XPS spectra recorded for thin film and powdered EH-IDTBR.

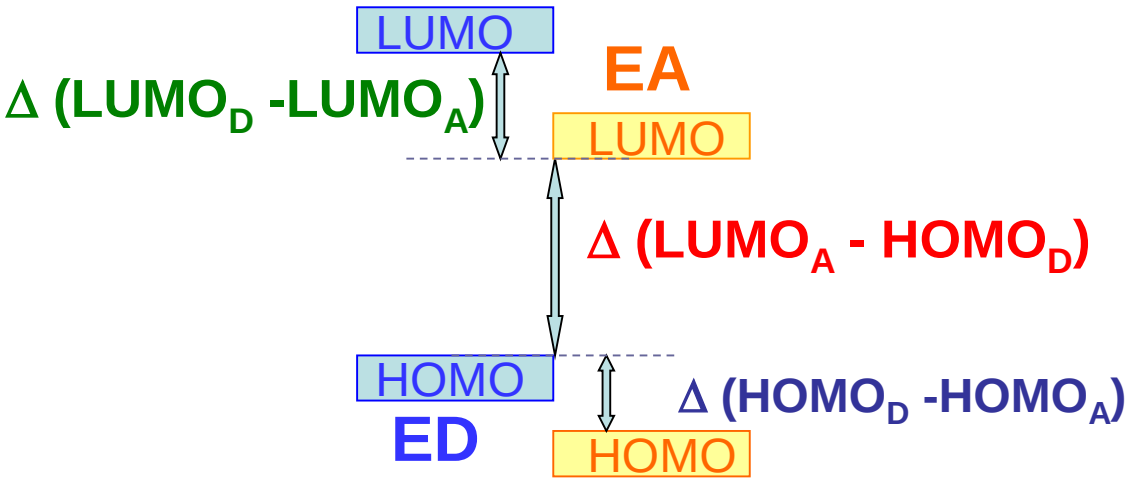

Figure 8: A schematic representation of the band structure of a contact E_D/E_A device.

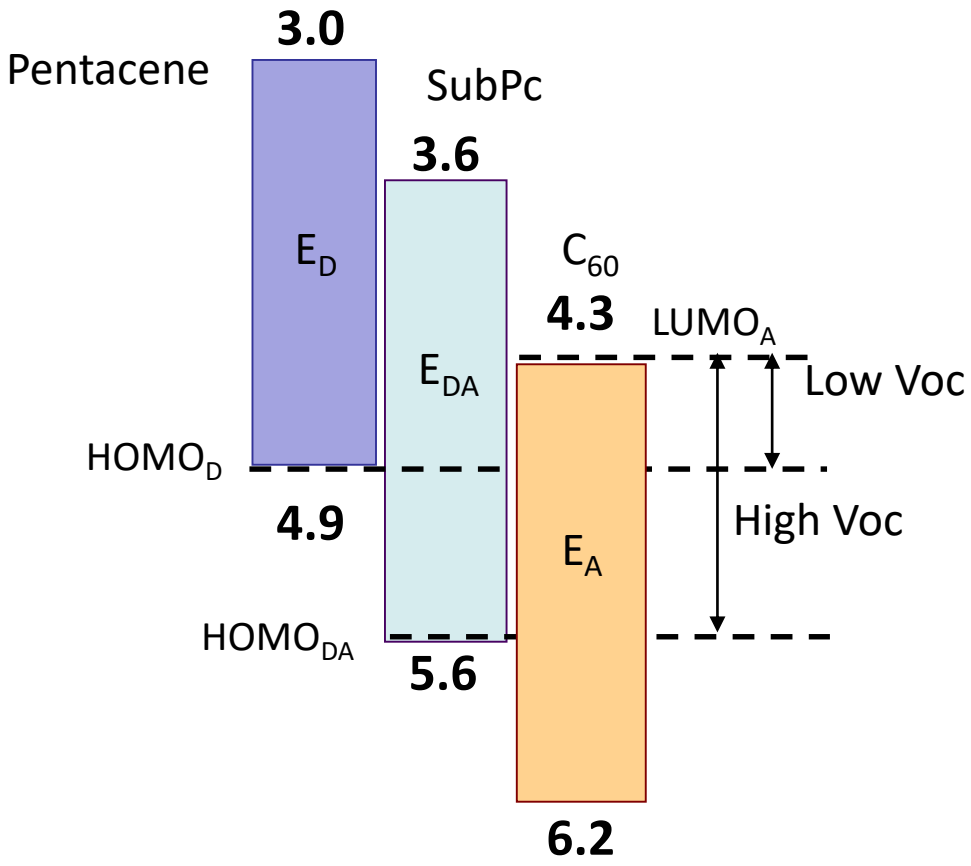

Figure 9: The band structure of the organic materials in a ternary OPVs using Pentacene/SubPc/C_{60}as an example.

Table 1: A summary of the parameters of the ternary OPV (Pentacene/SubPc/C_{60}) and its corresponding binary structures (* the HTL of this OPV is MoO_3/CuI, while it is MoO_3 for all the other OPVs presented in this table).

Sample (Thickness nm)	Voc (V)	Jsc (mA/cm^2)	FF (%)	η (%)
Pentacene(60)/SubPc (15)/C_{60}(40)	0.46	12.40	51	2.90
Pentacene(60)/SubPc (15)/C_{60}(40)*	0.41	9.50	43	1.70
SubPc (20)/ C_{60} (40)	1	5.33	49	2.63
Pentacene (60) /C_{60} (40)	0.43	7.96	58	1.98
Pentacene (60)/SubPc (15)	0.23	1.61	41	0.15

Table 2: Grain analysis and surface roughness parameters obtained for the different samples studied

Sample	Grain number/25 μm^2	Mean grain size (nm)	Total projected boundary length (µm)	Rq (nm)	Ra (nm)
ITO/MoO_3/pentacene	370	151	288	10.2	8.4
ITO/MoO_3/CuI/pentacene	870	109	347	6.0	4.8

Each analysis was performed from AFM images over a 5µm × 5µm area. The original data was plane-leveled to remove tilt by applying a numerical second-order correction. Particle analysis was carried out using the thresholding method (Gwyddion software).

Table 3: The LUMO and HOMO values of the different electron acceptors studied.

E_A	Pentacene	SubPc	C_{60}	PCBM[a]	EH-IDTBR[b]
LUMO	3.0	3.6	4.3	3.7	3.9
HOMO	4.9	5.6	6.2	6.1	5.7

[a][43].

[b][44].

Table 4: A summary of the parameters of the OPV prepared using the new E_A and its corresponding binary structures

Sample (thickness, nm)	Voc (V)	Jsc (mA/cm^2)	FF (%)	η (%)
Pentacene (60)/SubPc (15)/EH-IDTBR (4)	0.59	1.02	52	0.31
Pentacene (70)/)/EH-IDTBR (4)	0.43	0.58	59	0.15
SubPc (20)/EH-IDTBR (5)	0.94	2.45	24	0.55
Pentacene (60)/EH-IDTBR (4)/C60 (20)	0.49	3.28	43.5	0.7
Pentacene (60) /PCBM (41)	0.52	0.95	40	0.2
Pentacene (60) /SubPc 15/PCBM (20)	0.53	2.10	44	0.494

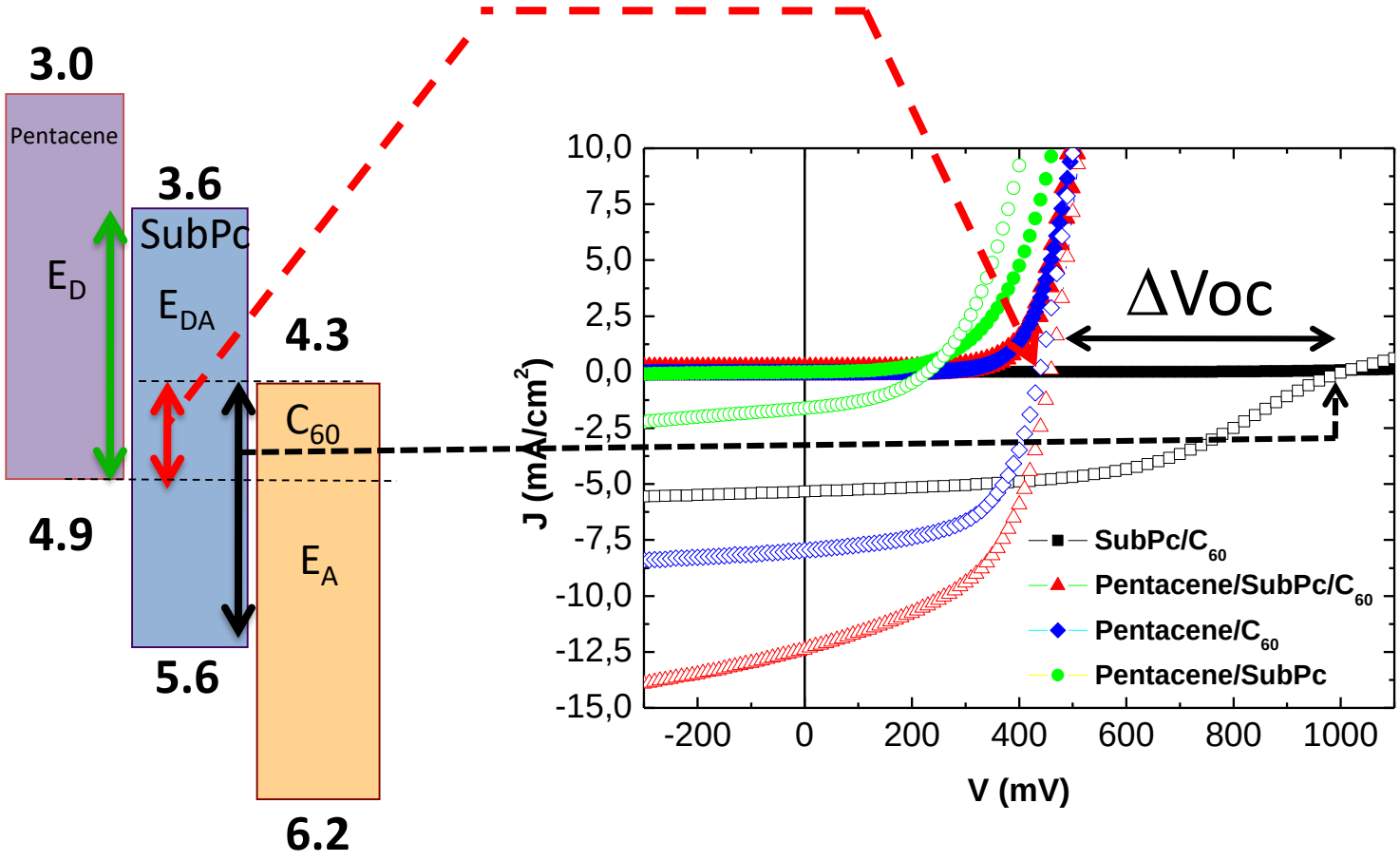
3.0
Pentacene
3.6
SubPc
E_D
E_DA
4.3
C60
E_A
4.9
5.6
6.2
ΔVoc
J (mA/cm²)
V (mV)
10,0
7,5
5,0
2,5
0,0
-2,5
-5,0
-7,5
-10,0
-12,5
-15,0
-200
0
200
400
600
800
1000
SubPc/C60
Pentacene/SubPc/C60
Pentacene/C60
Pentacene/SubPc